Landslides (2004) 1:29–40
DOI 10.1007/s10346-003-0008-7
Received: 29 September 2003
Accepted: 8 January 2003
Published online: 27 February 2004

A. Bichler · P. Bobrowsky · M. Best · M. Douma · J. Hunter · T. Calvert · R. Burns

Three-dimensional mapping of a landslide using a multi-geophysical approach: the Quesnel Forks landslide

Abstract A landslide located on the Quesnel River in British Columbia, Canada is used as a case study to demonstrate the utility of a multi-geophysical approach to subsurface mapping of unstable slopes. Ground penetrating radar (GPR), direct current (DC) resistivity and seismic reflection and refraction surveys were conducted over the landslide and adjacent terrain. Geophysical data were interpreted based on stratigraphic and geomorphologic observations, including the use of digital terrain models (DTMs), and then integrated into a 3-dimensional model. GPR surveys yielded high-resolution data that were correlated with stratigraphic units to a maximum depth of 25 m. DC electrical resistivity offered limited data on specific units but was effective for resolving stratigraphic relationships between units to a maximum depth of 40 m. Seismic surveys were primarily used to obtain unit boundaries up to a depth of >80 m. Surfaces of rupture and separation were successfully identified by GPR and DC electrical resistivity techniques.

Keywords Landslide · Mapping · Geophysics · 3-dimensional · Canada · British Columbia · Quesnel Forks

Introduction

The complex nature of many landslides necessitates the need for investigating their characteristics in as detailed a manner as possible (Bogoslovsky and Ogilvy 1977). To this end, it becomes important that the internal structure of the landslide and its surrounding environment be determined in order to facilitate reliable stability analyses and mitigation (Johnston and Ambos 1994; Bruno and Marillier 2000).

Models of landslide structure have traditionally been constructed based on geomorphic observations and when possible with the aid of limited subsurface data obtained by boreholes or excavations. Such direct methods (Hunt 1984) are more common but require labour intensive, and often costly, field work (Sharma 1997). During the past 20 years, advancements in computer processing and geophysical instrumentation have provided other means of collecting proxy data. Geophysical methods are considered indirect methods and provide non-destructive, portable techniques that can be used to cover large areas at relatively low costs (McGuffey et al. 1996). Still, geophysical surveys are rarely utilized to their full potential (Hack 2000). A comprehensive review of direct and indirect techniques is presented by Hunt (1984), Hutchinson (1984) and McGuffey et al. (1996) whereas Ogilvy (1974), Bogoslovsky and Ogilvy (1977), Goryainov et al. (1988), McCann and Forster (1990) and Hack (2000) describe geophysical techniques as applied to landslides.

The purpose of this paper is to present the results of a multi-parameter geophysical survey carried out on a landslide with the intention of mapping its internal structure. In addition it is shown that such integrated geophysical studies are effective in subsurface landslide investigation. The primary geophysical method used was direct current (DC) electrical resistivity, applied over a substantial portion of the landslide and adjacent terrain. Ground penetrating radar (GPR) and seismic surveys were also conducted, but over smaller areas. Geophysical data were calibrated against stratigraphic and surficial mapping and digital terrain models. The end result was the construction of an interpreted 3-dimensional structural model of the landslide.

Study area and the Quesnel Forks landslide

The landslide under investigation is located near the confluence of the Quesnel and Cariboo Rivers (52°40′ N, 121°40′W), near the eastern boundary of the Interior Plateau of British Columbia, Canada (Fig. 1). Local topography is characterized by a gently rolling plateau with an average elevation of 940 m a.s.l. near the landslide. East-west trending river valleys averaging 280 m in depth and 1.5 km in length incise the plateau. Climate data collected from Environment Canada stations for the period 1975 to 1993 show an annual temperature range between −39 and +35 °C and an average precipitation of 688 mm/year where approximately 480 mm is rain.

The Quesnel Forks landslide happened on April 28th, 1996 in the early morning and was witnessed by recreational campers at Quesnel Forks who reported hearing a loud rumble (Giesbrecht 2000). It occurred in a terrace opposite to the historical town site of Quesnel Forks (Fig. 2a). The terrace is 75 m high (Fig. 2b) and is bound to the north, east and west by the Quesnel River (Fig. 1). To the south, the terrace gives way to a steep bedrock-cored knob some 240 m high above the river. The terrace is primarily composed of sediment deposited during the last glaciation (Bichler 2003) and is underlain by bedrock of the Quesnel Terrane, related to a volcanic arc system (Bailey 1989). Phyllitic bedrock outcrops on the north side of the river and is assumed to underlie the terrace as well, though its depth is unknown.

The Quesnel River had a daily average discharge of 132 m^3/s for the period 1975 to 2002, measured at a gauge station 10 km upstream of the landslide maintained by Environment Canada. There are no major tributaries between the gauge station and the landslide. At the time of failure, during the onset of the spring flood, flow was 292 m^3/s, which is more than double the daily average flow for the preceding 9 months. Precipitation data are not available for the site at this time, though a station approximately 40 km to the southeast recorded no substantial rainfall preceding the event.

According to the classification of Cruden and Varnes (1996), the landslide was a retrogressive, dry earth slide-debris flow. The foot of the landslide extended across the river creating a type II landslide dam (cf. Costa and Schuster 1988). Subsequently the river breached the dam, partially eroding the foot of the landslide and the riverbank adjacent to the town. The duration of river

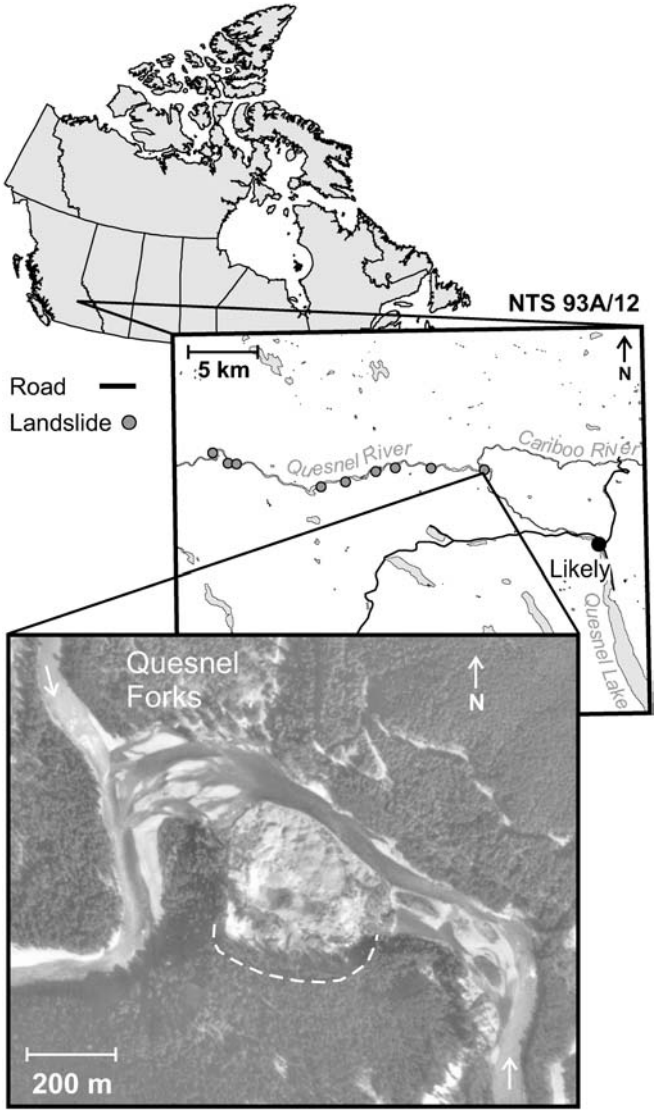

Fig. 1 Location map showing the National Topographic System (NTS) map sheet and orthophoto of Quesnel Forks. The *white dashed line* on the photo is the boundary of the head scarp

damming is unknown but was less than a few hours. River levels on the upstream side of the landslide remained 1 to 2 m higher at least several days after blockage (Klohn-Crippen Conslutants Ltd. 1996).

Evidence for prior instability of the terrace is known. In 1898 a landslide occurred upstream of a bridge formerly located at the base of the western edge of the terrace (Elliot 1996). By 1903 the road leading to the bridge required multiple relocations and by that time, approximately $10,000 (Canadian) had been spent in mitigation (Elliot 1996). Fear mounted that a major landslide could occur opposite Quesnel Forks endangering the town via a shift in river position (Wright 1987). The earliest aerial photos examined of the site from 1955 show a partially eroded foot of a relict landslide that protected the face of the terrace from fluvial erosion. This may be the remnant of the 1898 event. As evident from aerial photos, by 1970, the sediment was removed and erosion of the toe had started.

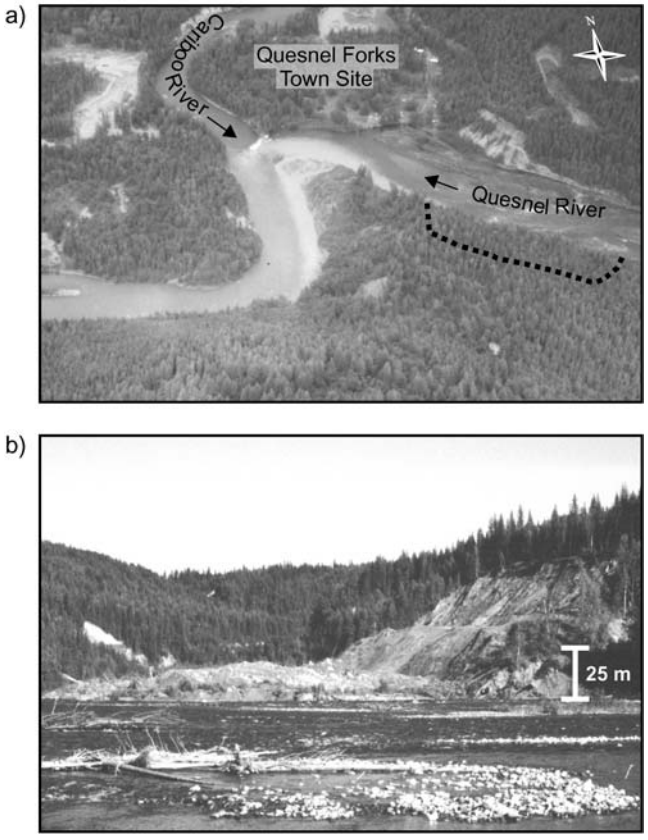

Fig. 2 **a** Pre-failure, oblique aerial photograph of Quesnel Forks taken the year prior to failure (1995). Note large amounts of silt being introduced into the Quesnel River. *Dotted line* shows the approximate location of the head scarp (photograph courtesy of Marie Elliot); **b** View to the southeast of the Quesnel Forks landslide, taken from the Quesnel Forks town site in 2001

Previous investigations of the landslide are limited to two site investigations focused on bank erosion caused by the landslide (Klohn-Crippen Consultants Ltd. 1996; Gottesfeld and Poirier 1999). Only brief descriptions of the landslide were included in these reports.

Methods

The investigation of the landslide involved several techniques including surficial mapping, stratigraphic and sedimentological studies, the creation of digital terrain models (DTMs) and geophysical surveys.

Initial efforts were directed towards the sedimentological and stratigraphic description of the landslide and terrace. Stratigraphic units were characterized using basic mapping methods from exposures along the escarpments of the terrace and the landslide. In addition, the contacts between units and other important topographical and structural features were surveyed for position and elevation using a laser theodilite station.

DTMs for both pre- and post-failure conditions were constructed from vertical aerial photographs taken in 1986 and 2002. The information was digitized at a scale of 1:1000. Topographic and cartographic data were then used to construct the surface of the DTMs and elevation change maps.

The geophysical methods applied at the site were GPR, DC electrical resistivity and seismic reflection and refraction. The

methods were chosen based on the expected characteristics of the landslide following reconnaissance geological mapping. All surveys were conducted during the late summer or early fall of 2002, which corresponds to the dry-season. This minimized the variability of geophysical results due to moisture differences (Bogoslovsky and Ogilvy 1977).

The GPR system used was the PulseEkko IV system from Sensors and Software. A 50-MHz antenna and receiver was chosen as a compromise between resolution and penetration depth. Ten metres of penetration is typical at this frequency (Annan and Cosway 1992) but depends strongly on the subsurface sediment characteristics. Resolution can be approximated by a fraction of the electromagnetic wave length, $\lambda/4$ to $\lambda/2$ (Sheriff 1984), and was calculated to be between 0.5 and 1 m assuming an average velocity of 0.1 m/ns for the electromagnetic wave. Two types of GPR surveys were conducted: reflection profiling to obtain pseudo-sections and expanding spreads or common mid-point for velocity analysis. All reflection surveys were carried out with a constant offset of 2 m between the transmitter and receiver. The measurement point is considered to be the mid-point between the transmitter and receiver. For this study a constant spacing of 0.5 m was used between measurement points. Velocity data were collected by expanding the separation between the transmitter and receiver about a central point in 1-m steps. The antenna and receiver were oriented perpendicular to the survey line for both types of surveys. Data processing was limited to topographic corrections based on surveyed elevations.

An IRIS Instruments SYSCAL R1-Plus Switch 48 DC electrical resistivity system was used for resistivity profiling. It is a 48-electrode system with the ability to select array types and collect multiple spreads. For survey lines longer than one spread of electrodes (48), the first 24 electrodes were moved to the end of the 48 electrode spread leaving electrodes 25–48 in their former positions for data collection in the new electrode array. This leapfrog approach was continued until the total line was covered. Electrode spacing was 5 m and the data were collected using a Wenner array configuration. Measurements were taken at a - spacings of 5, 10, 15, 25, 35, 45, 55, 65, and 75 m. Topographic corrections and 2-dimensional model inversions were preformed using Res2Dinv v3.4 software from GEOTOMO Software, which applies a least-squares method for determining the optimum inversion model (cf. Loke and Barker 1996).

Seismic surveys were conducted using a Geometrics SmartSeis R-48 seismograph. The system was a 48-channel instrument, although only 36 channels were used during the survey. Four types of surveys were carried out: (1) P-wave reflection, (2) P-wave refraction, (3) S-wave reflection, and (4) S-wave refraction. Geophones were spaced at 3-m intervals. P-wave surveys used 100-Hz vertical geophones whereas S-wave surveys used 8-Hz horizontal geophones mounted perpendicular to the survey line. A hammer seismic source was used for all surveys. A 16-lb hammer and 0.3-m section of I-beam was used for P-wave surveys whereas both the 16-lb hammer and I-beam and a 1.5-lb hammer and simple cylindrical rod were used for S-wave surveys. The direction of the S-wave source was also perpendicular to the line direction producing horizontally polarized (SH) shear wave energy. P-wave energy was minimized by reversing the S-wave source direction while simultaneously reversing the polarity of the received signal in the S-wave geophones. Reflection surveys were conducted using a 3-m spacing between shots. Refraction surveys had shot locations at both ends of the spread and in the centre. Data processing involved a combination of static and normal move-out corrections and the application of time domain and frequency domain filters.

The interpretation of geophysical units was based on internal characteristics, the orientation, depths, and geometries of contacts, stratigraphic descriptions, and knowledge of Quaternary and landslide processes. Depths of correlated units were then translated into a 3-dimensional model of the landslide and terrace.

Site characteristics

The following description of sediment and surficial material of the terrace and landslide is the result of reconnaissance mapping and provides the framework in which geophysical surveys were conducted. This information was then used to interpret the geophysical data in section 7.

Stratigraphy

The stratigraphy of the terrace is well exposed. The terrace consists primarily of sediment deposited during the Fraser Glaciation and is illustrated in a simplified column (Fig. 3). All stratigraphic units, except unit G, were deposited in association with advance outwash and a pro-glacial lake that formed when drainage of the Quesnel River valley became obstructed (Bichler 2003). Younger sediments were deposited but were subsequently removed by a combination of glacial and fluvial erosion.

The basal unit is laminated to finely bedded, well-compacted, silty sand and clay (unit A). The unit is not exposed at the landslide but was described from an outcrop located across the river and its presence inferred based on pre-failure photographs.

The lowest unit visible at the landslide consists of dipping, well-compacted, laminated sand that overlies crudely stratified

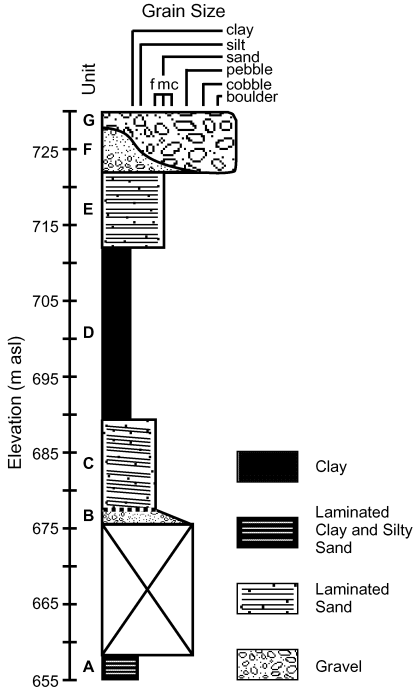

Fig. 3 Composite stratigraphic column for Quesnel Forks landslide

pebble gravel (units C and B, respectively). Unit B is at least 2.5 m thick whereas unit C is approximately 12 m thick. Sharply overlying this sediment is 22 m of moist, plastic clay with inclusions of fine sandy clay (unit D).

The remaining sediment consists of sand and gravel. Unit E is moderately compact, laminated sand up to 10 m thick. Unit F consists primarily of dipping, well-bedded, well-sorted, pebble gravel that is highly cemented and has an open framework. The unit is lenticular and up to 7 m thick. The upper most unit (unit G) consists of cobble, boulder gravel with a pebble and sand matrix, is up to 7 m thick, and forms the surface of the terrace.

Surficial characteristics

The distribution of surficial material is a product of the sediment comprising the terrace and the landslide. The ground conditions and surficial material are important because they affect the operation and effectiveness of geophysical surveys.

The terrace is heavily forested. The ground surface is flat and consists of a well-developed soil horizon that forms the forest floor. The southwest corner of the terrace is swampy. A rough road crosses the terrace from east to west.

The distribution of material over the landslide is complex. The upper translated block remains heavily forested (Fig. 4a). The forest floor remained intact during failure and is flat, including the surface of the road that shows no deformation. This is in contrast to the lower block that is largely bare of vegetation with a severely disturbed surface (Fig. 4b). Surficial material consists of sand and gravel from units F and G. The surface of the lower block is undulating.

The escarpment separating the upper and lower blocks is bare of vegetation. Its slope is approximately 40°. Primary stratigraphy is observed where the slope is steepest. A thick blanket of colluvium covers the surface where the slope is less steep. The surface of the escarpment separating the lower block from the foot of the landslide closely resembles the upper escarpment, though its slope is generally less steep, approximately 30°.

The foot of the landslide displays a variety of surficial materials and morphology. The most prevalent consists of hummocky clay or hummocky sand and gravel that can have local relief of more than 2 m (Fig. 4c; see also Fig. 5c). Near the centre of the foot, a splayed pattern consisting of pebble sand is present. The surface of the upstream (east) edge of the foot consists of well-sorted cobbles. The downstream (west) edge consists of fine-grained sand.

The volume of displaced material was estimated during surficial mapping, based on the geometry of the landslide. Assuming that the landslide has a typical spoon-shaped failure, the volume can be approximated by that of a half ellipsoid (Cruden and Varnes 1996) and was calculated to be 9.24×10^5 m^3.

In general, surficial conditions were well suited for carrying out geophysical surveys. In heavily forested areas, GPR and seismic surveys were conducted along roads to help facilitate data collection. The firm ground underlying the road offered better coupling for the GPR antenna and receiver as well as for the seismic energy source. Dry loose sand covered much of the slopes and is a poor electrical conductor, making it difficult to release sufficient energy into the ground during the resistivity survey. This also impeded the transfer of seismic energy into the ground and from the ground to the geophones, which is a common problem for seismic surveys conducted over landslides (Bruno and Marillier 2000). Lastly, the steep irregular landscape caused concern for collecting and interpreting the geophysical data because coupling between the geophysical transducers and the ground was difficult and complex corrections were required.

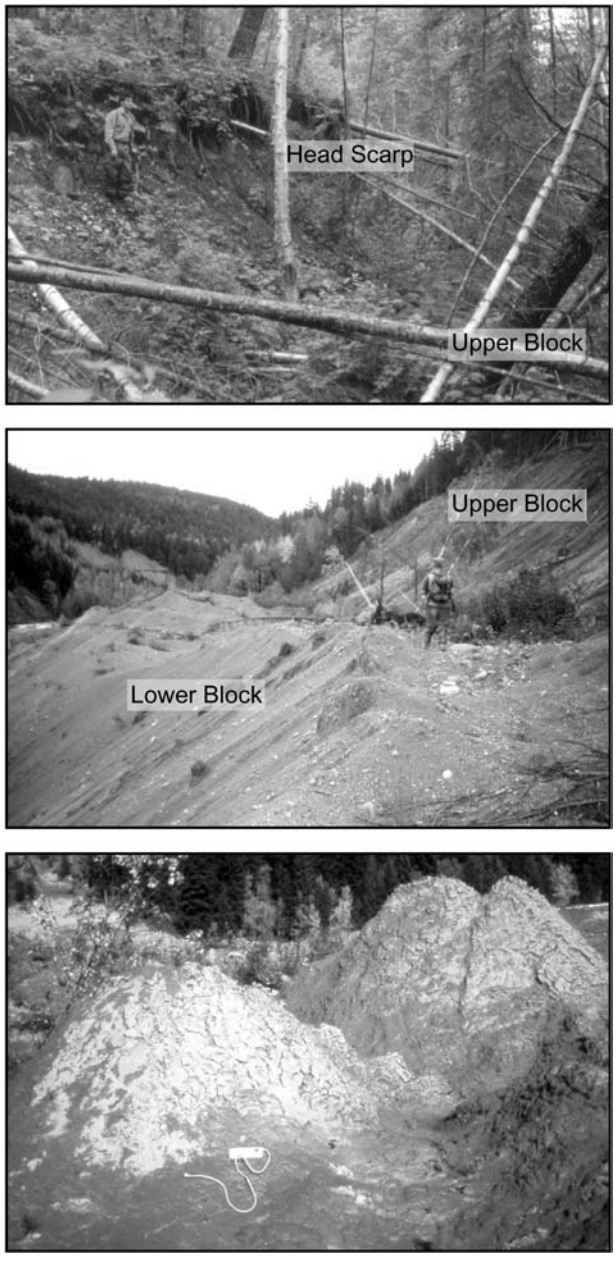

Fig. 4 **a** Disturbed forest floor near upper rotational block and head scarp, evident by the jack-strawed trees. Note the person standing on the headscarp for scale; **b** View to east along the top of the lower rotational block on which the person is standing; **c** Weathered clay blocks that create a hummocky surface over a portion of the foot. The *power bar* in the foreground is 25 cm in length

Digital terrain models

The DTMs record the pre- and post-failure geomorphology of the terrace and landslide (Fig. 5a, b, c and d). Along the northern edge of the terrace in the pre-failure DTM (Fig. 5a) a break in slope is evident and marks the future position of the head scarp (Fig. 5c). The face of the terrace was steep, especially at river level.

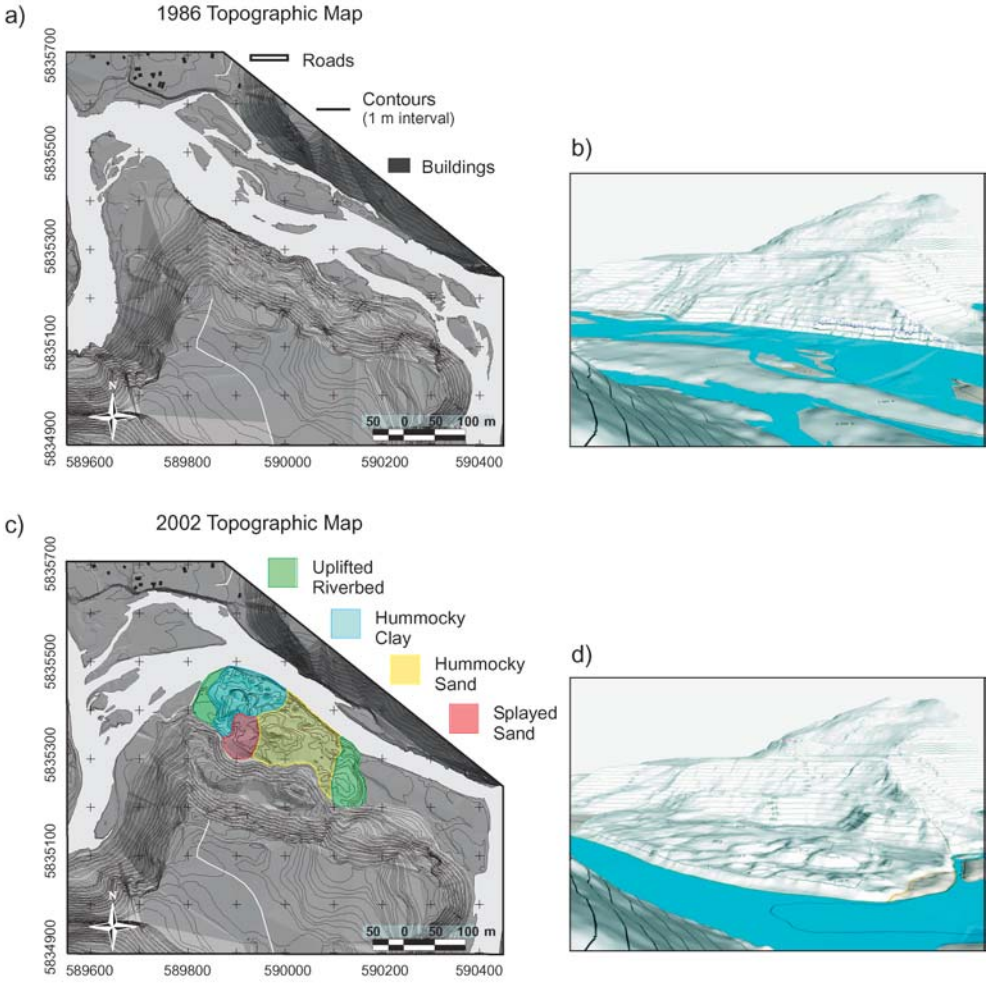

Fig. 5 Digital terrain models of the Quesnel Forks landslide and surrounding area: **a** Pre-failure shaded relief map; **b** Pre-failure 3D oblique view to southeast; **c** Post-failure shaded relief map with morphological division of foot (see section 6.2); and **d** Post-failure 3D oblique view to southeast

The post-failure DTM shows the general morphology of the landslide, shift in river position, and erosion of the northern bank of the Quesnel River affecting the town site.

An elevation change map was created based on these models (Fig. 6). Vertical displacements for the upper and lower blocks are 6 and 50 m, respectively. The DTMs were also used to calculate the net volume change. The area defined by a decrease in volume is the depletion and has a loss equal to approximately 5.3 x 10^5 m^3. Conversely, the area with a net gain in volume is the accumulation and is approximately 3.6×10^5 m^3. This discrepancy is discussed in section 8.

Geophysical results

Using the three geophysical methods described in section 4, 28 profiles were generated: 7 GPR, 12 DC electrical resistivity, and 9 seismic (Fig. 7). Several profiles that characterize the most important features of each method have been selected for discussion. The interpretation and relation of geophysical data to stratigraphic data are then presented in the following section (section 9).

Ground penetrating radar

A total of 340 m of GPR reflection profiles were acquired. Two profiles are presented, A-A' and B-B', which have a maximum

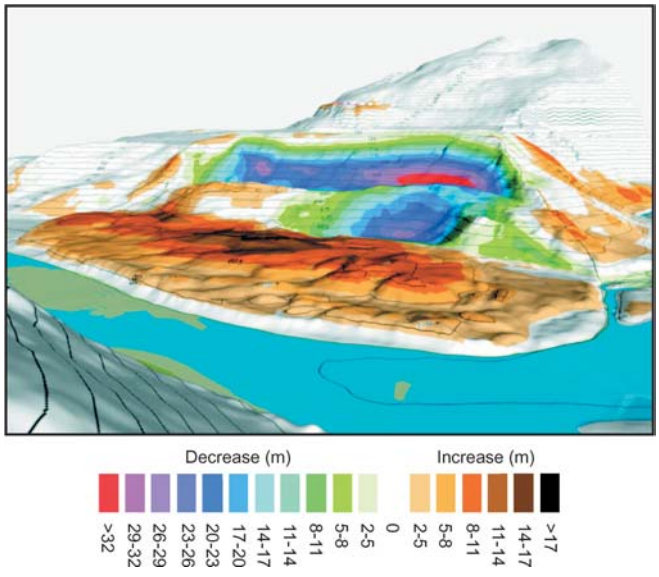

Fig. 6 3D oblique change of elevation map created from DTMs. *Brown shades* indicate an increase in elevation from the 1986 to the 2002 aerial photo. *Green*, *blue* and *red shades* represent a decrease in elevation. View is to the southeast

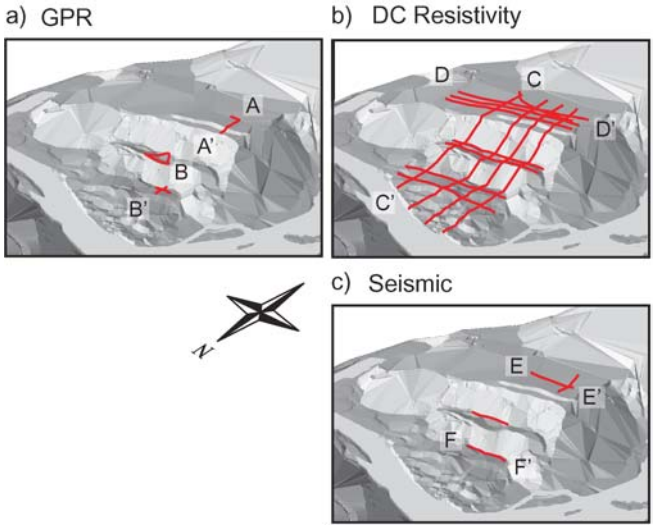

Fig. 7 DTMs with geophysical survey lines superimposed onto its surface: **a** GPR; **b** DC electrical resistivity; and **c** Seismic reflection and refraction. Profiles obtained from corresponding survey lines are discussed in sections 6.1, 6.2, and 6.3 of the text

penetration depth of approximately 25 m (Fig. 8a and b, respectively). Both are perpendicular to the head scarp and run north–south (Fig. 7a). Profile A-A' was conducted along the road on the terrace and ends at the edge of the upper block. No data were collected from 52 to 62 m due to the steep face of the head scarp. Profile B-B' begins at the escarpment of the lower block and extends away from the head scarp. Depths for profiles were calculated assuming a constant velocity of 0.1 m/ns, as determined from velocity analysis.

A total of 7 radar facies are identified. Dipping or hummocky reflectors characterize the upper two facies in both profiles and form the upper 8 to 12 m (facies 1, 2, 5 and 6). Individual reflectors are up to 1.5 m thick. Beneath are subhorizontal, coherent, and laterally extensive reflectors (facies 3 and 7). In profile A-A', facies 3 is approximately 14 m thick. The thickness of facies 7 in profile B-B' is indeterminate. A fourth facies (facies 4) in profile A-A' is identified by a weak, continuous horizontal reflector that marks its upper contact.

Two steeply dipping reflectors are recognized within the upper block that cross cut radar facies and that do not define facies boundaries (Fig. 8a). The first event has an apparent dip of 40° to the north (solid red line). It offsets facies boundaries and reflectors. The second event has an apparent dip of 45° to the south (dashed green line) with no evidence of offset.

Direct current electrical resistivity

A total of 4,100 m of profiles were collected during the resistivity survey. Two profiles are presented, C-C' and D-D' (Fig. 9a, b, respectively). The mean depth of investigation for the DC resistivity surveying technique is primarily a function of the largest spacing between electrodes and is calculated to be 39 m using Edwards (1977). Profile C-C' is perpendicular to the head scarp and extends from the terrace to the tip of the foot whereas profile D-D' is parallel to the head scarp on the terrace (Fig. 7b).

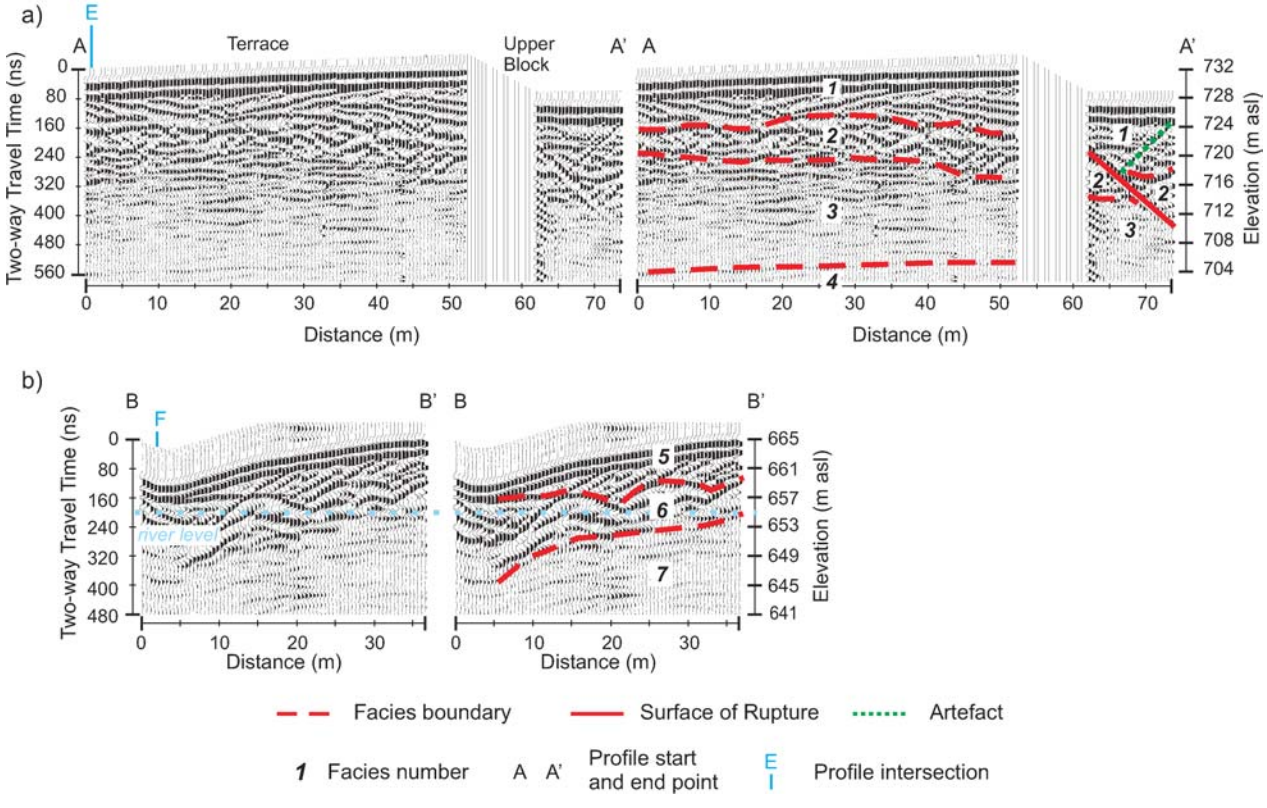

Fig. 8 GPR profiles (both interpreted and uninterpreted), corresponding with profiles in Fig. 7: **a** Perpendicular to head scarp on terrace and upper block (*A-A'*); and **b** Perpendicular to head scarp on foot (*B-B'*)

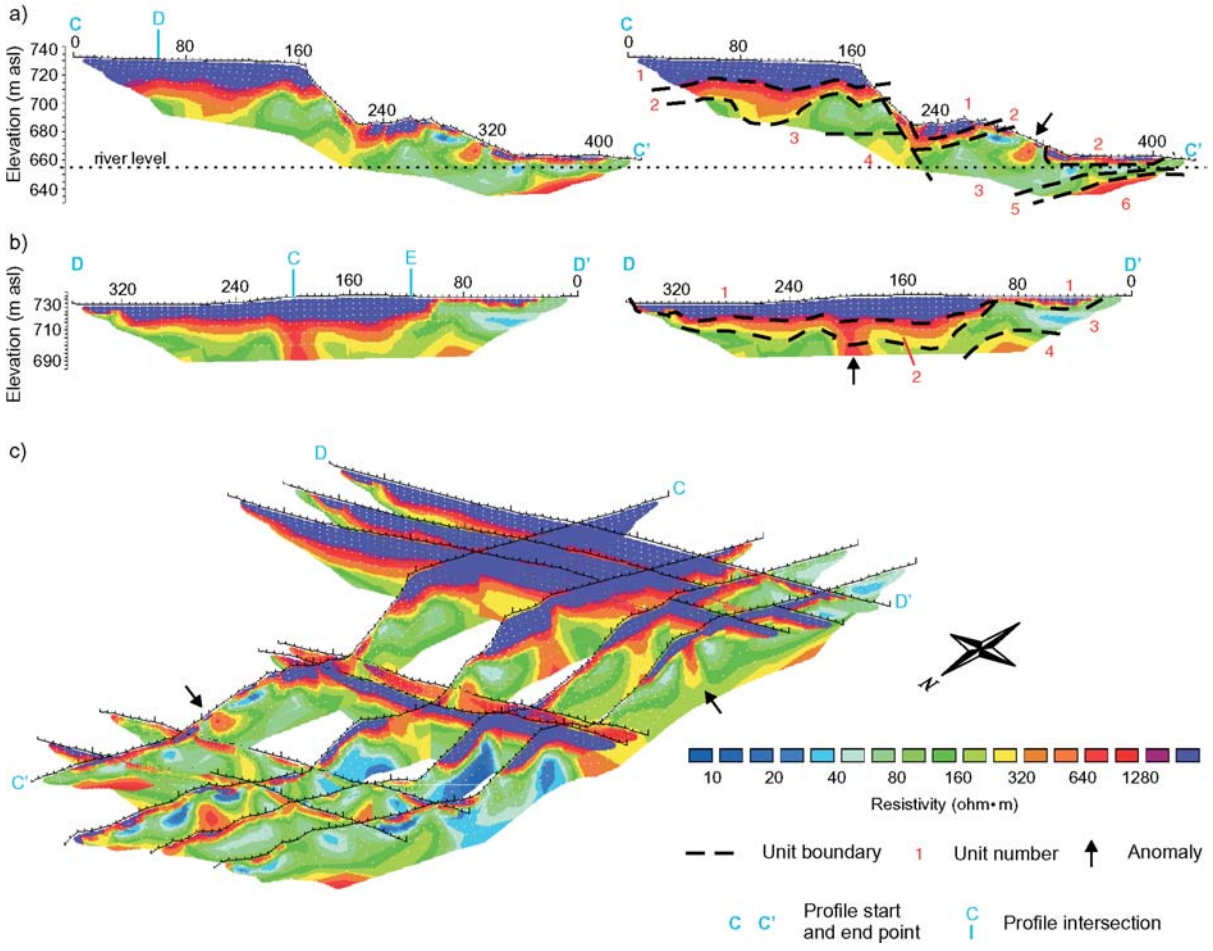

Fig. 9 DC electrical resistivity profiles (both interpreted and uninterpreted), corresponding with profiles in Fig. 7: **a** Perpendicular to head scarp (*C-C'*); **b** Parallel to head scarp (*D-D'*); and **c** 3D fence diagram of all resistivity data

In addition, all the resistivity data collected are illustrated in a 3-dimensional fence diagram (Fig. 9c).

Six resistivity units are identified from the data, each with its own range of resistivities. Some resistivity values within a given unit are outside the ranges of the unit, a result of processing or high topographic relief. Units 1 and 2 have high resistivity values ≥960 ohm m and 240 to 960 ohm m, respectively. They are found near-surface and are thickest under the east side of the terrace, approximately 35 m. Both disappear toward the southwest. These units are comparably thin and discontinuous over the landslide. A third highly resistive unit (unit 6) is found below the foot and has a resistivity range between 640 to 1,280 ohm m. Its upper contact dips 20° toward the valley centre (south) with no basal contact evident.

The least resistive unit (unit 3 with resistivity values <120 ohm m) is found both beneath the terrace and landslide. Within the terrace it is up to 30 m thick. The unit underlies units 1 and 2, except in the southwest where it comes to surface. Under the landslide it is up to 40 m thick and is thickest below the lower block.

Units 4 and 5 have considerable overlap in their resistivity values, 120 to 640 ohm m and 60 to 320 ohm m, respectively. Unit 4 is >20 m thick and is found beneath the terrace whereas unit 5 ranges from 5 to 10 m thick and is found below the foot (Fig. 9a).

Seismic reflection and refraction

A total of 852 m of profiles were collected using seismic methods. Reflection profiles E-E' and F-F' (Fig. 10a and b respectively) are both parallel to the head scarp (Fig. 7c). Profile E-E' is a P-wave reflection profile collected along the road on the terrace. The deepest reflector identified is roughly 80 m below surface whereas the shallowest is 15 m. Profile F-F' is an S-wave reflection profile collected on the foot of the landslide. The deepest reflector from this profile is 30 m deep and the shallowest 20 m deep.

Eight seismic units were identified. Seven units are present in the terrace on Profile E-E' with units 6, 7 and an additional unit (unit 8) in the foot of the landslide on Profile F-F'. In profile E-E', reflectors are roughly parallel with the upper three units thickening to the east. The thickest unit bounded by an upper and lower reflector is unit 6, thickening from 20 to 30 m to the west. The second thickest is unit 3, which thickens from 7 to 20 m to the east. An estimated P-wave velocity of 1,450 m/s was chosen for calculating the depth scale based on velocity analysis. Unit 6 is the only unit bound by two reflectors and is approximately 8 m thick for profile F-F'. If unit 8 extends to surface, it is 22 m thick. The depth scale for this profile was calculated using an estimated S-wave velocity of 250 m/s, also based on velocity analysis.

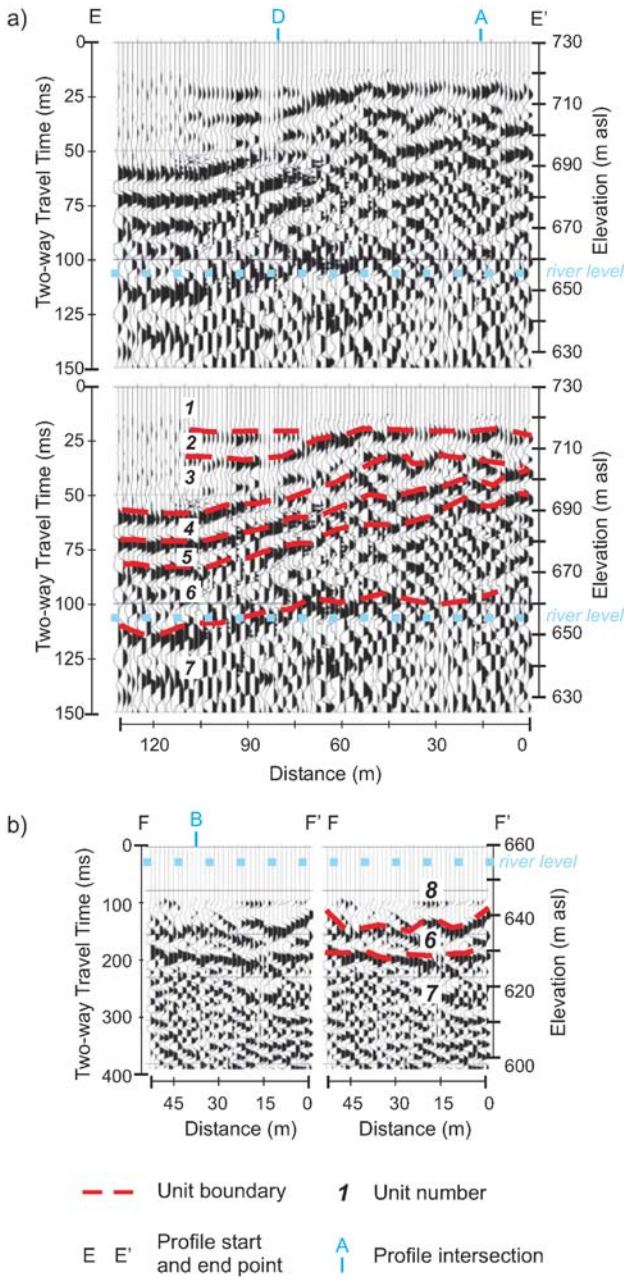

Fig. 10 Seismic profiles (both interpreted and uninterpreted), corresponding with profiles in Fig. 7: **a** Parallel to headscarp on the terrace (P-wave reflection) (*E-E'*); **b** Parallel to headscarp on the foot (S-wave reflection) (*F-F'*)

Geophysical interpretation

Surficial and stratigraphic mapping is combined with geophysical data to create a 3-dimensional cut-away model of the Quesnel Forks landslide (Fig. 11). Typical ranges of geophysical parameters (resistivity, P- and S-wave velocities, dielectric constant or radar velocity) for material similar to those described in section 6 are given in Table 1 and are used in the interpretations. The characteristics of the terrace are addressed first and are represetative of the pre-failure state of the material involved in the landslide (cf. McCann and Forster 1990). Interpretations of the displaced material follow.

The terrace is composed of 8 geophysical units or layers that are nearly horizontal. Seven of the layers are correlated to stratigraphic units described in section 4.1. The upper gravel units (G and F) are correlated to radar facies 1 and 2, respectively, and seismic and resistivity unit 1 (Fig. 11). GPR data show that the terrace gravels (unit G) consists of channel structures whereas the cemented gravels (unit F) consist of hummocky beds. The high resistivity values and the P-wave velocity obtained by refraction surveys (501 m/s) are indicative of dry sand and gravel (Table 1).

The upper laminated sand (unit E) is interpreted as resistivity and seismic unit 2. It is absent from the GPR profile A-A' because it disappears towards the west as shown in profiles D-D' and E-E' (Figs. 9b and 11a). Resistivity values are slightly less than for the overlying gravel, which is reasonable especially if the sand has greater moisture content.

The appearance of laminated sand corresponds to an abrupt thickening of coarse-grained units in the east part of the terrace (Fig. 10b). This may reflect the preference of the ancestral Quesnel River to erode less consolidated sand and gravel rather than more competent units. The laminated sand and gravel units comprise a succession of porous sediment that are likely permeable (cf. Fetter 2001).

Clay (unit D) is interpreted as radar facies 3, which shows substantial internal structure contrary to stratigraphic descriptions. This suggests that the pockets of sand contained within unit D have a more coherent structure than previously recognized. This unit is also correlated with resistivity and seismic unit 3 (Fig. 11). Resistivity values are low and are typical of clay (Table 1). A refraction survey yielded a P-wave velocity of 1,502 m/s and is also suggestive of fine-grained, water-saturated sediment. Resistivity profiles show that he unit comes to surface to the southwest (Fig. 9c) and because clay is relatively impermeable, this explains the presence of surface water.

Though the penetration of GPR signals is normally rapidly attenuated in clay, a weak reflection from the base of the clay unit is evident and marks the contact with the lower laminated sand unit (C). The sand is thus correlated with radar, resistivity, and seismic unit 4 (Fig. 11). Like the upper laminated sand unit, resistivity values are less than the gravel units, but greater than those of clay.

The lower gravel unit (unit B) is correlated with seismic unit 5 (Fig. 11). An equivalent radar facies is absent because the unit lies below the effective penetration depth of the GPR system. It is also absent from resistivity data. Two possible reasons exist: it may not differ sufficiently in electrical properties from the overlying sand or it is too thin to be detected as a separate unit at this depth. In either case, it is incorporated into resistivity unit 4.

The interbedded, silty sand and clay (unit A) is assumed to underlie the lower gravel unit (B) and is correlated with seismic unit 6 (Fig. 11). This in turn overlies bedrock (seismic unit 7) which is the deepest reflector seen in the terrace. Both units lie below theeffective penetration depths for GPR and resistivity methods.

Geophysical data within the displaced blocks of the landslide resemble those of the terrace with a few exceptions. The upper coarse-grained units are thinner and show signs of deformation, particularly in the western half of the lower block where the units have partially slid off the block (Fig. 9c). Measurements of the orientation of unit boundaries in the east half of the lower block indicate that units underwent approximately 12° of back rotation

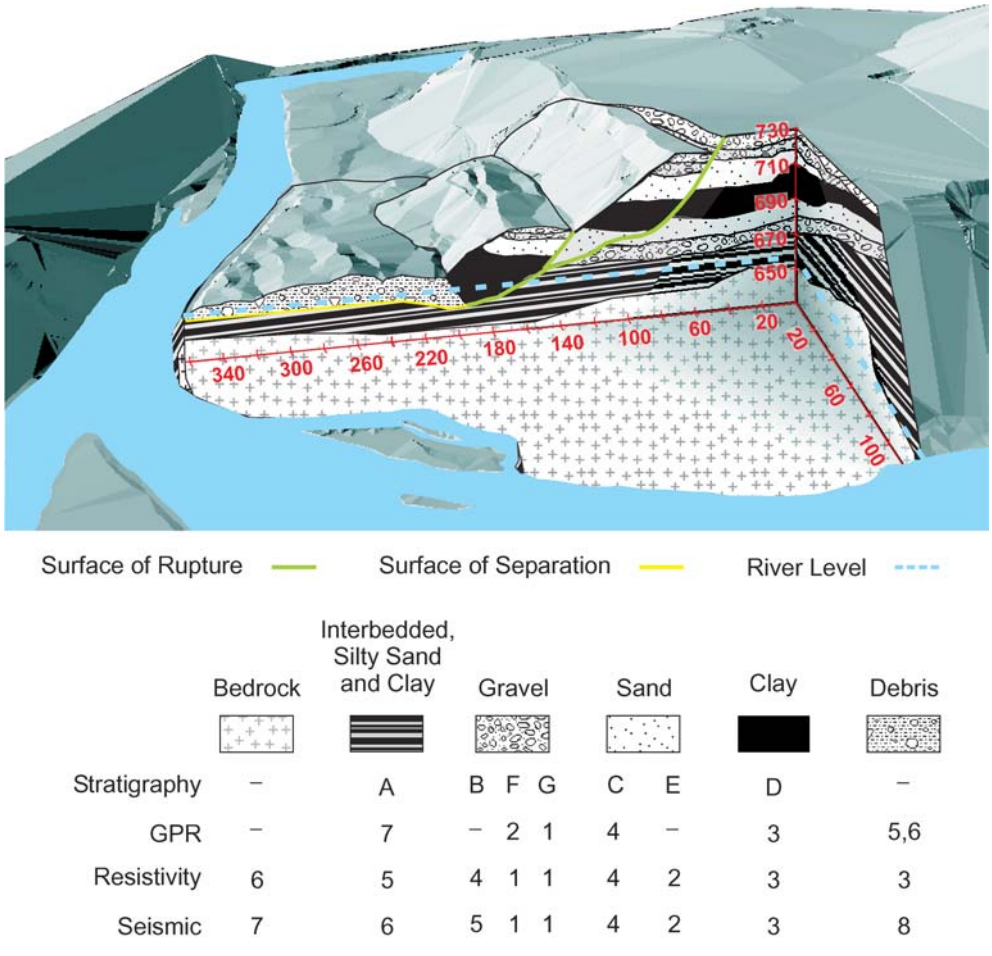

Fig. 11 An oblique, 3D cut-away model of the Quesnel Forks landslide based on geophysical data. Geophysical units are correlated stratigraphic units in the accompanying matrix. Elevation is given in metres above sea level and distance in metres

Table 1 Geophysical parameters of various substrates used during the interpretation of geophysical data

Substrate	Seismic Vp (m/s) (Lankston1990; Sharma1997)	Seismic Vs (m/s) (Lankston1990)	Resistivity (Ωm) (Ward1990; Sharma1997)	GPR V (m/ns) (Davis and Annan1989; Sharma1997)
Air	330			0.30
Water (fresh)	1,400–1,500		4–100	0.03
Alluvium, sand (dry)	300–1,000		1–1,000	0.15
Sand and gravel	1,050	520	800–10,000	0.09–0.15
Sand	500–1,300	300–570	800–5,000	
Sand (water saturated)	1200–2,200	540		0.06
Silt				0.07
Clay	730–2,500	390–410	1–120	0.05–0.17
Glacial moraine	1,500–2,600		8–4,000	

(Fig. 9a). A third difference is that resistive unit 3 is thicker and is not underlain by resistive units seen in the terrace. As such, the lower sand and gravel units (B and C) are thought to be absent below the block. These units were likely remobilized during failure and are incorporated into the foot of the landslide. It is believed that the unusual thickness of unit 3 is due to the loss of resolution at depth that leads to the electrical indifference between displaced clay (unit D) and adjacent interbedded, silty sand and clay (unit A).

Separating the blocks from the terrace is the rupture surface; thus is imaged with both GPR and resistivity surveys. The northward dipping reflector in profile A-A' represents the rupture surface for the upper block (Fig. 8a, solid red line). Displacement is approximately 5.5 m in the vertical direction, measured from the upper contact of the cemented gravel unit (facies 2). This agrees with measurements based on the DTMs, approximately 6 m. In addition, beds along this surface show deformation indicative of a downward motion of the upper block. The second dipping surface is interpreted as an artefact created by the reflection of a surface wave from the edge of the block at the sediment-air interface (Fig. 8a, dashed geen line).

The rupture surface below the lower block is seen in resistivity profiles where displacements lead to the juxtaposition of electrically contrasting units. This is illustrated in profile C-C' (Fig. 10a)

where gravel, sand and clay (units 1, 2, and 3) are found adjacent to laminated sand (unit 4). The rupture surface dips approximately 60° to the north and lessens to 45° to the west. Total vertical displacement is 40 m as measured from the offset of the upper contact of the clay unit, though this is about 10 m less than observations from the DTMs.

Two radar facies (5 and 6), two resistivity units (2 and 3) and one seismic unit (8) make up the displaced material within the foot (Fig. 11). The upper facies in GPR profile B-B' masks underlying topography and is composed of a series of reflectors that dip into the head scarp (Fig. 8b, facies 5). This unit corresponds to pebbly sand identified during surficial mapping as being splayed over the foot. The parent material is interpreted to be the cemented pebble gravel (unit F) though the origin of the internal structure is unknown. The sediment was likely deposited when a block disintegrated on impact with the foot of the landslide.

Much of the foot consists of radar facies 6, which is correlated with resistivity unit 3 (Fig. 11). It is composed of hummocky beds of low resistivity typical of clay (Table 1) but has layers of contrasting material that generate the strong reflectors seen in the GPR data. The unit is composed of material mobilized by flow. As such, resistivity unit 3 is correlated to two separate lithological units: the clay found within the terrace and blocks and the material within the foot (Fig. 11).

Radar facies 7, resistivity unit 5 and seismic unit 6 are correlated with the interbedded, silty sand and clay (unit A) (Fig. 11). Radar data indicate that the unit has sub-horizontal bedding consistent with stratigraphic descriptions. Resistivity values for the unit are slightly greater than for clay or disturbed material from within the foot. Even so, it remains conductive, which is evident by the strong attenuation of the GPR signal. Because the unit is not deformed, the upper contact is interpreted as the surface of separation and is correlated to the contact between resistivity units 3 and 6 and seismic units 8 and 6 (Fig. 11). This surface displays undulations perpendicular to flow, is deepest nearest the toe of the lower block, approximately 20 m, and shallows away from the head scarp.

The area consisting of cobble gravel along the eastern edge of the foot (Fig. 6c) is known to directly overlie an undisturbed stratum (resistivity unit 5). The sediment bears a strong resemblance to lateral bars found in the river near the landslide and is interpreted as a displaced part of the riverbed. The fine-grained, relatively flat area along the western edge of the foot may also be a part of the river or was deposited as a back channel when the river began to erode the foot of the landslide.

Using the surfaces of rupture and separation to define the boundary of displaced material, an estimation of the volume was made. Through this method, approximately 1.7×10^6 m^3 of material was displaced.

Resistive unit 6 is interpreted as bedrock. This is supported by the presence of bedrock on the north side of the river, adjacent to the foot. As such, seismic unit 7 also represents bedrock and can be seen beneath the terrace as well as the foot (Fig. 10). The data show that bedrock dips towards a central point located under the landslide.

Discussion

From this study it was found that the most useful data for mapping the terrace and landslide in three dimensions was that obtained using resistivity mapping. This was primarily the result of the higher density of data collection. Seismic and GPR data could not so easily be collected on the slopes as resistivity data mainly because of coupling problems. Bogoslovsky and Ogilvy (1977) suggest that at least 3 profiles along the axis of the landslide and several perpendicular to it be conducted and should extend beyond the limits of the landslide. Additionally, the resistivity survey offered a compromise between shallow high-resolution (GPR) and deep low-resolution (seismic) techniques. These other geophysical methods proved useful for extending interpretations beyond the limits of the resistivity data.

The excellent exposure of stratigraphy at surface and along escarpments provided the basis for interpreting geophysical data. Survey lines conducted directly over these exposures yielded data that correlate well with geophysical parameters and stratigraphic units. Furthermore, good correlation exists between data from different geophysical techniques where survey lines crossed or were coincident. An example is the intersection of resistivity line D-D' and seismic line E-E' where the upper contact of the clay unit (resistivity and seismic unit 3) is determined to be approximately 20 m and 22 m below surface, respectively (Figs. 9b and 11a). Elsewhere, GPR line A-A' crosses seismic line E-E' where the same contact has depths of approximately 10 and 12 m, respectively (Figs. 8a and 11a). A high degree of correlation also exists for survey lines conducted by the same method. An exception is the variance seen in resistivity data, though this variation occurs primarily within the respective range of a unit and therefore contact boundaries are unaffected. Note that resistivity values have the largest range of any geophysical parameter and logarithmic variations are common within a given resistivity unit.

The rupture surface for the upper block is best imaged by the GPR method. The reflection of the GPR signal by this surface suggests that material has contrasting geophysical properties (i.e. dielectric constant), likely brought about by shearing. It is possible that this boundary is also evident in the resistivity data but the presence of resistivity variations attributed to the inversion process impedes a reliable conclusion (Fig. 9c). In contrast, the rupture surface of the lower block is best imaged by the resistivity method and is visible because of contrasting resistivity values of lithological units brought about by emplacement during failure. The surface itself has no uniquely identifiable electrical properties at the resolution of the survey conducted. Like the rupture surface, the surface of separation is also identifiable by the geophysical methods due to its contrasting geophysical properties across the boundary but has no unique properties itself.

The volume of the landslide was calculated by three different methods. Calculations based on DTMs are not representative of the total volume of displaced mass. Instead they are an estimate of displaced material relative the original ground surface. It estimated the lowest volume: more than three times lower than the volume calculated using the geophysical data. A problem inherent to volumes based on DTMs is that no account is taken of the depth of water, in this case the amount of material deposited into the river channel. This is partially responsible for the discrepancy between the volume of the depletion and accumulation. An additional factor is the erosion of material from the foot by the river that is common to calculations based on geophysical data as well. The volume obtained by field observa-

tions and a simplified geometry of the landslide estimates the total volume of displaced mass and represents the second highest volume. It is still half of the volume estimated using the geophysical data. The volume calculated using the geophysical data is considered to be the best approximation and thus further emphasizes the importance of these methods in landslide mapping.

The 3-dimensional model of the terrace and landslide constructed from the geophysical data aids in the understanding of landslide processes. Though no slope stability analysis was attempted, some general statements can be made based on the results of this investigation. (1) The presence of a thick succession of coarse-grained sediment overlying clay may have led to the formation of a perched water table that would have increased pore water pressure within underlying clay unit and therefore decreased the effective strength of that unit. The perched water table may have also increased shear stresses within the terrace. These sediments thicken towards the east and would have concentrated groundwater in this region. (2) The rupture surfaces penetrate all stratigraphic units except the interbedded, silty sand and clay (unit A). Within this unit the surface shallows. (3) The role of bedrock is negligible as it is found at a substantial depth beneath the boundaries confining the landslide.

Conclusions

The suite of geophysical techniques employed over the Quesnel Forks landslide has proved to be a valuable tool for subsurface investigations of unstable slopes. The multi-geophysical survey approach resulted in a more detailed and less ambiguous interpretation of the 3-dimensional structure of the landslide and terrace than if any one geophysical method were used in isolation. The variance of scales of resolution and penetration and geophysical parameters was important since no one method was ideal for characterizing the environment.

The choice of DC electrical resistivity as the primary method for mapping was appropriate given the electrical contrasts and geometry of strata and the target depths. Penetration to approximately 40 m was achieved. Ground penetrating radar helped resolve near-surface structures (up to approximately 25 m depth) whereas seismic methods provided structural information for greater depths (approximately 80 m).

Geophysical data collected show a close correlation with units identified by each of the perspective methods as well as to the observed stratigraphy. This allowed the construction of a reliable 3-dimensional model. It shows sub-horizontal units of unconsolidated sediment overlying bedrock within the terrace. Two displaced blocks of sediment are identified and consist of a succession of similar units. These sediments have undergone relatively little deformation and maintain the integrity of their original characteristics. The material comprising the foot has undergone extensive deformation and no longer resembles the primary stratigraphy. The boundaries separating the displaced material from undisturbed strata were also identified.

From this model, it is suggested that increased pore water pressures in the clay unit and artificial loading of terrace due to a perched water table played a role in the instability of the terrace but was not necessarily the trigger. It is much more likely that fluvial erosion of the terrace face was responsible for the loss of shear strength and subsequent collapse of the terrace. Similar to the landslide that occurred in 1898, the foot of the Quesnel Forks landslide protects the terrace from erosion and will likely do so for many years.

Acknowledgements

The Geological Survey of Canada has provided the primary funding for this research with secondary funding from the British Columbia Geological Survey Branch. In addition, the GPR unit was kindly supplied by the British Columbia Ministry of Transportation. The authors thank Adrian Hickin, Roger Paulen, Katie Dexter, Nicole Vinette, Paul Grant and Hart Bichler for their invaluable contributions in the field. This project has also benefited from collaboration with Marten Geertsema of the Ministry of Forests. Digital terrain models were produced by McElhanney Consultants Ltd. and elevation change maps and associated volume calculations were conducted by Geosolutions Ltd.

References

Annan AP, Cosway SW (1992) Ground penetrating radar survey design. Sensors and Software, Mississauga

Bailey DG (1989) Geology of the hydraulic map area, NTS 93A/12. British Columbia Ministry of Energy, Mines and Petroleum Resources, Victoria

Bichler (2003) Landslides, stratigraphy and surficial geology of the hydraulic map sheet (NTS 93A/12). MSc Thesis, School of Earth and Ocean Sciences, University of Victoria, Victoria

Bogoslovsky VA, Ogilvy AA (1977) Geophysical methods for the investigation of landslides. Geophysics 42:562–571

Bruno F, Marillier F (2000) Test of high-resolution seismic reflection and other geophysical techniques on the Boup landslide in the Swiss Alps. Surv Geophys 21:333–348

Costa JE, Schuster RL (1988) The formation and failure of natural dams. Geol Soc Am Bull 100(7):1054–1068

Cruden DM, Varnes DJ (1996) Landslide types and processes. In: Turner AK, Schuster RL (eds) Landslides investigation and mitigation, Spec Rep 247, Transportation Research Board, National Research Council, Washington

Davis JL, Annan AP (1989) Ground-penetrating radar for high-resolution mapping of soil and rock stratigraphy. Geophys Prosp 37:531–551

Edwards LS (1977) A modified pseudosection for resistivity and induced-polarization. Geophysics 42:1020–1036

Elliot M (1996) Quesnel Forks: slides 1898 and 1996. British Columbia Historical News 29(4):2–3

Fetter CW (2001) Applied hydrogeology. Prentice Hall, Upper Saddle River

Giesbrecht BD (2000) Quesnel Forks restoration project. Restoration Project Committee of the Likely and District Chamber of Commerce, Likely

Goryainov NN, Matveev VS, Varlarnov NM (1988) Use of geophysical methods for landslide and mudflow investigations. In: Kozlovskii YA (ed) Landslides and mudflows. UNESCO, Moscow

Gottesfeld AS, Poirier RW (1999) Quesnel Forks historic townsite: Erosion Protection Project. Quesnel River Enhancement Society

Hack R (2000) Geophysics for slope stability. Surv Geophys 21:423–338

Hunt RE (1984) Geotechnical engineering investigation manual. McGraw-Hill, New York

Hutchinson JN (1984) Methods of locating slip surfaces in landslides. Bull Assoc Eng Geol 20(3):235-252

Johnston JJ, Ambos EL (1994) Three-dimensional landslide structure for seismic refraction data analysis: a case study from Blind Canyon, northern Santa Ana Mountains, California. Society of Exploration Geophysicists Annual Meeting, Society of Exploration Geophysicists, Tulsa

Klohn-Crippen Consultants Ltd (1996) Quesnel Forks, Erosion Assessment, R. Rodman, Richmond

Lankston RW (1990) High-resolution refraction seismic data acquisition and interpretation. In: Ward SH (ed) Geotechnical and environmental geophysics. Review and tutorial. Soc Explor Geophys Tulsa

Loke MH, Barker RD (1996) Rapid least-squares inversion of apparent resistivity pseudosections by a quasi-Newton method. Geophys Prosp 44:131–152

McCann DM, Forster A (1990) Reconnaissance geophysical methods in landslide investigations. Eng Geol 29:59–78

McGuffey VC, Modeer VA, Turner AK (1996) Subsurface exploration. In: Turner AK, Schuster RL (eds) Landslides investigation and mitigation, Spec Rep 247, Transportation Research Board, National Research Council, Washington
Ogilvy AA (1974) Current trends in the use of geophysical methods in the study of landslide phenomena. Moscow University Geology Bull 29(4):48–50
Sharma PV (1997) Environmental and engineering geophysics. Cambridge University Press, New York
Sheriff RE (1984) Encyclopedic dictionary of exploration geophysics. Soc Explor Geophys Tulsa
Ward SH (1990) Resistivity and induced polarization methods. In: Ward SH (ed) Geotechnical and environmental geophysics. Review and tutorial. Soc Explor Geophys Tulsa
Wright RT (1987) Quesnel Forks: a gold rush town in historical perspective. Friends of Barkerville Historical Society, Barkerville

A. Bichler (✉)
University of Victoria,
School of Earth and Ocean Sciences,
PO Box 3055, Victoria, BC, V8W 3P6, Canada
e-mail: bichler@geo.uni-erlangen.de

P. Bobrowsky · M. Douma · J. Hunter · T. Calvert · R. Burns
Natural Resources Canada,
Geological Survey of Canada,
601 Booth St., Ottawa, ON, K1A 0E8, Canada

M. Best
Bemex Consulting International Ltd.,
5288 Cordova Bay Rd.,
V8Y 2L4, Victoria, BC, Canada